Published in final edited form as:
J Mol Cell Cardiol. 2009 November ; 47(5): 603–613. doi:10.1016/j.yjmcc.2009.07.030.

Cell Therapy Enhances Function of Remote Non-Infarcted Myocardium

Alicia Moreno-Gonzalez[1,5], **F. Steven Korte**[1,5], **Jin Dai**[1], **Kent Chen**[3,4], **Bryan Ho**[1], **Hans Reinecke**[2,4], **Charles E. Murry**[1,2,4], and **Michael Regnier**[1,4]

[1] Department of Bioengineering, University of Washington, Seattle WA 98195 USA

[2] Department of Pathology, University of Washington, Seattle WA 98195 USA

[3] Department of Medicine/Cardiology, University of Washington, Seattle WA 98195 USA

[4] Centers for Cardiovascular Biology, Institute for Stem Cell and Regenerative Medicine, University of Washington, Seattle WA 98109 USA

Abstract

Cell transplantation improves cardiac function after myocardial infarction; however, the underlying mechanisms are not well-understood. Therefore, the goals of this study were to determine if neonatal rat cardiomyocytes transplanted into adult rat hearts one-week after infarction would, after 8-10 weeks: 1) improve global myocardial function, 2) contract in a Ca^{2+} dependent manner, 3) influence mechanical properties of remote uninjured myocardium and 4) alter passive mechanical properties of infarct regions. The cardiomyocytes formed small grafts of ultrastructurally maturing myocardium that enhanced fractional shortening compared to non-treated infarcted hearts. Chemically demembranated tissue strips of cardiomyocyte grafts produced force when activated by Ca^{2+}, whereas scar tissue did not. Furthermore, the Ca^{2+} sensitivity of force was greater in cardiomyocyte grafts compared to control myocardium. Surprisingly, cardiomyocytes grafts isolated in the infarct zone increased Ca^{2+} sensitivity of remote uninjured myocardium to levels greater than either remote myocardium from non-treated infarcted hearts or sham-operated controls. Enhanced calcium sensitivity was associated with decreased phosphorylation of cTnT, tropomyosin and MLC2, but not changes in myosin or troponin isoforms. Passive compliance of grafts resembled normal myocardium, while infarct tissue distant from grafts had compliance typical of scar. Thus, cardiomyocyte grafts are contractile, improve local tissue compliance and enhance calcium sensitivity of remote myocardium. Because the volume of remote myocardium greatly exceeds that of the grafts, this enhanced calcium sensitivity may be a major contributor to global improvements in ventricular function after cell transplantation.

Corresponding Authors: Michael Regnier, Ph.D., University of Washington, Department of Bioengineering, Institute for Stem Cell and Regenerative Medicine, Box 355061, Seattle, WA 98195-7962 USA, Phone (206) 616-4325, Fax (206) 685-3300, mregnier@u.washington.edu; Charles E Murry, MD, PhD, University of Washington, Departments of Pathology and Bioengineering, Center for Cardiovascular Biology, Institute for Stem Cell and Regenerative Medicine, 815 Mercer St, Brotman 453, Seattle, WA 98109, Phone (206) 616-8685, Fax (206) 897-1540, murry@u.washington.edu.
[5]These authors provided equal contribution to this work

Disclosures: None

Keywords

Myocardial Infarction; Cardiomyocytes; Phosphorylation; Myofibrillar Proteins

Introduction

Cell-based therapies for cardiac repair hold great promise for the treatment of myocardial infarction. It has been demonstrated that transplantation of many cell types (including cardiomyocytes) into experimentally induced myocardial infarctions improves myocardial performance as assessed by decreased cavity dilation, increased ejection fraction, decreased infarct expansion, and increased developed systolic pressure [1-6]. These encouraging results have led to the initiation of several clinical trials (reviewed in reference [7]). Very little is known, however, about the mechanism by which cell transplantation improves heart function. In fact, at least seven general mechanisms have been hypothesized in the literature: re-muscularization, attenuated post-infarct ventricular remodeling, paracrine effects leading to increased angiogenesis or to increased survival of cardiomyocytes near the infarct border zone, immunomodulation of the infarct environment, improvements in the extracellular matrix, and recruitment of resident cardiac progenitors[7]. Thus, the underlying mechanisms by which cell-based therapies can contribute to the improvement of myocardial performance clearly warrant investigation.

The overall design of this study was to investigate the active and passive mechanical properties of transplanted cells and host myocardium as a means to determine the cellular-tissue basis of improved whole-heart function following cell transplantation. Neonatal rat cardiomyocytes (NRCs) were grafted into the infarct region of adult rat hearts one week following permanent occlusion of the left anterior descending coronary artery to address four main questions: (1) can transplanted cells contract in a Ca^{2+} dependent manner similar to normal myocardium, thus having the potential to re-muscularize the damaged region? (2) can transplanted cells reduce the stiffness of damaged myocardium, thus improving diastolic behavior? (3) do transplanted cells influence the mechanical properties of myocardium remote from the injury site? and (4) are there potential myofibrillar mechanisms that may explain the mechanical differences observed?

Materials and Methods

More extensive details of Methods are provided in the online data supplement.

Cell Preparation and Animal Model

These studies were approved by the University of Washington (UW) Animal Care Committee and were conducted in accordance with federal guidelines. Animals were housed in the Department of Comparative Medicine at the UW and were cared for in accordance with the US NIH Policy on Humane Care and Use of Laboratory Animals. Neonatal rat cardiomyocytes (NRCs) were isolated from 1-3-day old newborn syngeneic Fischer 344 rats and Di-I labeled as described in the data supplement. The surgical procedure for coronary occlusion of adult rat hearts and graft injection was as previously described [8-10].

Echocardiography

Echocardiography was performed as described by Laflamme *et al* [11]. Rats were lightly sedated with isoflurane and monitored by continuous electrocardiography (ECG) via three limb leads. Echocardiographic measurements were taken using a GE Vivid7 echocardiography system with an 11 MHz convex transducer of parasternal long axis and short-axis images at

the mid-papillary muscle level to ensure evaluation of the infarcted region of the hearts. M-mode measurements on the short-axis view were taken to obtain left ventricular end-diastolic (LVEDD) and systolic dimensions (LVESD). Fractional shortening (FS) was calculated as (LVEDD-LVEDS)/LVEDD × 100%. Measurements were made on at least three cardiac cycles by two blinded echocardiographers and averaged for each data value.

Strip Dissection and Mechanical Measurements

Dissected hearts were Vibratome-sliced and demembranated (by Triton) overnight at -20°C to remove the sarcolemmal and sarcoplasmic reticulum membranes [12]. Graft regions were identified by visualization of the CM-DiI label under a fluorescent microscope. Strips were dissected manually and connected via aluminum T-clips to pin hooks on a force transducer and linear motor in a mechanical setup similar to one previously described [13] for active and passive force measurements. Following mechanical measurements the samples were processed for histology and western blotting as detailed in the online supplement.

SDS-PAGE, Western Blotting, Histology, and Transmission Electron Microscopy

Primary antibodies used were against α-myosin heavy chain (α-MHC) (ATCC, clone BA-G5, Manassas, VA), β-MHC (ATCC, clone A4.591, Manassas, VA), cardiac troponin I (cTnI) (HyTest, Turku, Finland), slow skeletal TnI (ssTnI) (Santa Cruz Biotechnology, Santa Cruz, CA), TnT (Sigma, St. Louis, MO), and sarcomeric actin as a loading control (Sigma, St. Louis, MO). Secondary antibodies were conjugated to peroxidase for chemiluminescence and were: sheep anti-mouse-IgG (GE Healthcare, Buckinghamshire, UK) for α-MHC, β-MHC, cardiac troponin T (cTnT), and cTnI; bovine anti-goat-IgG (Santa Cruz Biotechnology, Santa Cruz, CA) for ssTnI; goat anti-mouse-IgM (Sigma, St. Louis, MO) for sarcomeric actin. Pro-Q Diamond staining (Invitrogen, Eugene, OR) was performed as previously described [14]. UV transillumination was used to visualize and digitally record phosphoprotein bands, and then the gel was washed overnight (25% methanol/10% acetic acid), restained with for total protein content with Coomassie blue, and scanned for digital recording. The Pro-Q Diamond phosphoprotein band areas were densitometrically determined using ImageJ (NIH) and normalized to actin density. Strips were prepared for immunostaining after mechanical measurements and stained with picrosirius red and fast green cytoplasmic stain. Percent collagen area was quantified from images taken under linearly polarized light by number of picrosirius red-positive pixels divided by total number of tissue strip pixels. Transmission electron microscopy (TEM) was performed following overnight fixation in half-strength Karnovsky's fixative (2.0% paraformaldehyde, 2.5% glutaraldehyde, 0.1M cacodylate buffer, 3mM $CaCl_2$, pH 7.3).

Statistical Analysis

Values are shown as mean ± S.E.M., unless indicated otherwise. ANOVA test was used on each measurement among all groups to determine significant differences, with followed by Student-Neuman-Keuls t-tests post-hoc. (SigmaStat). Differences at the p-value < 0.05 were considered statistically significant.

Results

In vivo functional assessment

Example echocardiography recordings are shown in Figure 1A-C and measurements for all hearts are summarized in Figure 1D-E. Fractional shortening (FS) was significantly increased in grafted hearts (MI+NRCs) (24.5 ± 2.6 %, n = 10) compared to non-treated (MI+vehicle) infarcted hearts (15.7 ± 1.0 %, n = 9) ($p < 0.05$, Figure 1D) at 8-10 weeks post-treatment, in agreement with previous studies [4, 15-17]. However, both groups had depressed function

compared to sham operated (non-infarcted) hearts (FS = 44.6 ± 2.0 %, n = 6). Grafted hearts had reduced left-ventricular (LV) end-systolic dimension (LVSD; 5.5 ± 0.3 mm) compared to non-treated infarcted hearts (6.4 ± 0.2 mm, $p < 0.05$), but this was still larger than for non-infarcted hearts (3.3 ± 0.2 mm) (Figure 1E). LV diastolic dimension (LVDD) was significantly larger in all infarcted hearts compared to non-infarcted ($p < 0.05$), irrespective of treatment. We noted no arrhythmia in infarcted hearts via limb-lead ECG irrespective of treatment. Overall, these results demonstrate that NRC grafts, while not large enough to restore normal function, significantly improved the function of infarcted hearts.

Transmission electron microscopy

Transmission electron microscopy of the grafted tissue 8 weeks after transplantation showed capillaries containing red blood cells, indicating vascularization of the graft. Grafted cardiomyocytes were, in general, differentiated, but with some important differences from host myocardium (Figure 2). Grafted cells contained abundant mitochondria densely packed amongst the myofibrils (Figure 2B). The myocytes were rod-shaped and aligned uniaxially, with clearly evident intercalated discs between grafted cells, containing desmosomes, adherens junctions and gap junctions. T-tubules associated with sarcoplasmic reticulum were observed in the grafts, indicating development of mature cardiomyocytes. The principal difference from host cardiomyocytes (Figure 2A, C) was some misalignment of the Z-discs in grafted cells, which may influence active mechanical properties. Additionally, while grafted cell myofibrils were organized into sarcomeres with defined M-lines, A- and I-bands (Figure 2D), there appeared to be an expanded A band, a reduced I band width, and a minimal H band. This indicates that these cells are somewhat less mature than sham, but more mature than neonatal cardiomyocytes. Overall, this provides evidence that injected cardiomyocytes can integrate and mature even when isolated within the context of scar tissue.

Ca^{2+} Activated Force

To examine the contractile properties of graft tissue and its effect on uninjured (remote) myocardium we measured the Ca^{2+} dependence of steady-state force and the maximal rate of force redevelopment (k_{tr}) in demembranated tissue strips. Successful engraftment of pre-labeled (CM-DiI positive) NRCs was confirmed by gross morphology during tissue dissection for mechanical measurements (Figure 3A-E) and by immunostaining heart tissue sections (Figure 3F-I). Figure 3F-I shows a typical graft eight weeks after cell transplantation as identified by CM-DiI (red). Sarcomeric actin (green) identified grafted cells as primarily cardiomyocytes (Figure 3G). Importantly, and by design, transplanted cells did not have significant zones of direct physical contact with uninjured host myocardium and were surrounded by a distinct area of hypo-cellular, CM-DiI negative scar tissue. This allowed the assessment of whether grafted cells could survive in isolation and develop towards the adult cardiomyocyte phenotype, independent of direct contact with host myocardium. Although occasional instances of graft cells in contact with border zone non-infarcted myocardium were observed, this tissue was not used for mechanical measurements.

Values for all tissue dimension and contractile properties are summarized in Table 1 and selected data are shown graphically in Figure 4. All cardiomyocyte grafts demonstrated clear force development in the presence of activating levels of Ca^{2+}, whereas no force developed in infarct strips from media-injected hearts. Normalized maximal force (F_{max}) and maximal k_{tr} for NRC grafts were ~11% and 55% of control strips, respectively, but were similar to values from neonatal tissue (Figure 4B-C). Grafts had no influence on F_{max} or maximal k_{tr} of remote tissue. Graft and neonatal strips had a similar Ca^{2+} sensitivity of force (pCa_{50} = 5.69 ± 0.07, n=6 and 5.70 ± 0.06, n=7, respectively), while both showed greater Ca^{2+} sensitivity than sham strips (5.41 ± 0.03, n=14) or trabeculae (5.39 ± 0.04, n=7) (Figure 4D-E). The greater Ca^{2+} sensitivity of neonatal vs. adult rat myocardium (+0.29 pCa units) is similar to previously

reported values [18,19]. Interestingly, we found that the Ca^{2+} sensitivity of force for remote myocardium from grafted hearts (pCa_{50} = 5.64 ± 0.10, n=7) was much greater than for remote myocardium from non-treated infarcted hearts (pCa_{50} = 5.45 ± 0.04, n=12) or tissue strips from sham-operated hearts (Figure 4E). Importantly, this suggests that transplanted cells can enhance the active mechanical properties of myocardium remote from the grafted area of infarcted hearts.

Myofilament Protein Characterization

Myofilament protein isoform content and phosphorylation profiles were characterized to correlate with tissue mechanical properties (Figure 5). Myosin heavy chain (MHC) isoform is a principal determinant of the rate of force redevelopment and power output in striated muscle [20,21], and the higher β-MHC in neonatal rat myocardium [18] is suggested to result in a slower rate of force development than for adult tissue (which contains predominantly α-MHC [22]). Western blot analysis showed that NRC graft tissue contained high levels of β-MHC with no detectable levels of α-MHC (Figure 5A). This likely explains the slower k_{tr} in the grafts compared with control tissue and remote tissue from infarcted hearts (Figure 4C, Table 1). Tissue from sham-operated hearts and remote tissue from infarcted heart had mostly α-MHC and only small amounts of β-MHC, which correlates with their faster k_{tr} values (Figure 4C, Table 1). Thus, both k_{tr} and western blot analysis suggest grafts did not greatly influence MHC isoform expression in remote tissue of infarcted hearts.

Slow skeletal TnI (ssTnI) is expressed in neonatal rat myocardium and transitions to cardiac TnI (cTnI) in adult myocardium[19] in association with decreased Ca^{2+} sensitivity in adult myocardium. To determine if the increase in Ca^{2+} sensitivity observed in both NRC grafts and remote myocardium from grafted hearts was due to a greater level of ssTnI expression in myofilaments, we assessed the content of cTnI and ssTnI by western blotting (Figure 5B). We found that cTnI was the predominant isoform in all of the samples from adult hearts (including graft tissue), with ssTnI detectable only in neonatal myocardium (from 1-2 or 3-4 day old animals). Thus, it appears that NRC grafts completely converted to cTnI expression by 8 weeks after transplantation, even though myosin isoform remained unchanged. Thus, myofilament TnI isoform composition cannot explain the greater Ca^{2+} sensitivity of force for grafts and remote myocardium from grafted hearts.

Myofilament protein phosphorylation is a key regulator of cardiac function and is known to change dramatically following myocardial infarct and during the progression to heart failure [14,23-25]. To determine if altered myofilaments protein phosphorylation could account for differences in Ca^{2+} sensitivity of force, SDS-PAGE was performed and gels were stained for phosphoproteins using Pro-Q-diamond. There was an overall decrease in myofilament phosphorylation in all infarcted groups as compared to sham (Figure 5E). Interestingly, however, remote tissue from grafted hearts had significantly less phosphorylation of troponin T (TnT), tropomyosin (Tm), and myosin light chain 2 (MLC-2) as compared to remote tissue from non-treated, infarcted hearts (Figure 5C-E). There was no difference in myosin binding protein C (MyBP-C) between groups or in TnI phosphorylation (the two major myofilament targets for cAMP-dependent protein kinase (PKA)) between remote tissue from infarcted hearts receiving NRC grafts vs. non-treated infarcted hearts. There was also no difference between groups in an unidentified phospho-band located above TnT (~60 kDa). On the other hand, TnT and MLC-2 are phosphorylated by protein kinase C (PKC), and this phosphorylation is thought to reduce and enhance the Ca^{2+} sensitivity of contractile force, respectively, with TnT phosphorylation exerting the dominant affect [26]. Thus, reduced phosphorylation of TnT and/or MLC-2 could explain the increased Ca^{2+} sensitivity of force observed in remote tissue from grafted hearts. Tm phosphorylation has only recently come under investigation, but could have significant effects due to the key role it plays in steric regulation of myosin binding.

Phosphorylation of TnT, Tm, and MLC-2 was also significantly lower in NRC grafts compared with tissue from sham-operated hearts and remote tissue from infarcted hearts, and were similar to remote tissue from grafted hearts (Figure 5E). This suggests that the phosphorylation level of these myofilament proteins may account, at least in part, for a greater Ca^{2+} sensitivity of force in NRC grafts as well.

Passive Mechanical Properties

To determine tissue stiffness, passive force (stress) of myocardial strips was measured during a series of stretches between 0% and 20% of initial strip length (Figure 6A,B). This range likely assesses the contribution of collagen (as opposed to titin) to the stiffness of the tissue (see Discussion). Scar tissue from animals that received either NRC grafts ($K = 4676 \pm 1380$ mN/mm^2, n=5) or vehicle ($K = 3730 \pm 1340$ mN/mm^2, n=9) was an order of magnitude stiffer than any of the other groups ($p < 0.05$ vs. control). Strikingly, graft strips ($K = 453 \pm 156$ mN/mm^2, n=8) exhibited approximately the same stiffness as sham myocardium ($K = 273 \pm 100$ mN/mm^2, n=4) (Figure 6C). This suggests that cell grafts reduced wall stiffness, but only in the regions of the infarct containing the graft itself. Neonatal myocardium was considerably less stiff ($K = 39 \pm 9$ mN/mm^2, n=17) ($p < 0.05$ vs. sham control), correlating with a previous study reporting porcine neonatal myocardium was less stiff than adult myocardium [27]. The stiffness of remote myocardium from animals that received either NRC grafts ($K = 596 \pm 213$ mN/mm^2, n=12) or vehicle ($K = 469 \pm 76$ mN/mm^2, n=11) was not significantly different from sham strips or trabeculae ($K = 586 \pm 217$ mN/mm^2, n=7), suggesting that transplanted cells do not affect the passive mechanical properties of remote myocardium.

Stress relaxation of passive tension was investigated to determine if the viscoelastic properties of graft strips were also similar to normal myocardium. The time constant of force decay following stretch to 1.2 L_o (t50d = time to reach 50% decay force) was used as a measure of the visco-elastic component of myocardial tissue (arrow in Figure 6A). Interestingly, passive force in grafts decayed faster ($t50d = 1.3 \pm 0.3$ s, n=8) than in any other type of strip ($p < 0.05$ vs. sham) Decay constants ranged from 1.9-4.1 seconds in other strip types, none of which differed significantly from one another (Figure 6D). This indicates that, although stiffness *per se* is similar in grafts compared to normal myocardium, the viscoelastic properties of the graft are clearly altered. More rapid elastic recoil in grafts compared to neonatal or adult myocardium or scar tissue suggests a distinction in the cellular/molecular mechanism responsible for establishing and maintaining their passive stiffness.

Collagen Content

To determine if the passive properties were correlated with differences in collagen Type I content, we quantified the histological area of tissue strips that stained positive for collagen with picrosirius red (Figure 7) [28]. Most noteworthy, graft strips contained significantly lower percent collagen content (43.5 ± 4.4, n=11) as compared to scar strips (62.9 ± 4.1, n=5) ($p < 0.01$). However, this 31% reduction in collagen seems unlikely to explain the 10-fold difference in passive stiffness. Moreover, graft strips still contained significantly more collagen than any other group except scar, yet had statistically similar passive force and stiffness values than myocardial strips. These data, along with t50d results (see above and Figure 6), suggests that graft strips have a unique stress-strain phenotype. Neonatal strips contained the lowest percent collagen content of all the groups (0.8 ± 0.2, n=5), in agreement with reported values [29,30]. The percent collagen area in remote myocardium from grafted (6.0 ± 3.0, n=4) or non-treated infarcted hearts (2.1 ± 1.2, n=4) did not differ from each other or from that found in sham strips (3.1 ± 0.3, n=4) ($p < 0.05$), suggesting NRC grafts do not affect the collagen content of remote myocardium.

Discussion

In the present study, we characterized the active and passive mechanical properties of neonatal rat cardiomyocyte (NRC) grafts and their influence on uninjured remote myocardium 8-10 weeks after transplantation into adult rat hearts (one week after infarction). We report the novel findings that NRC grafts appear to mature by morphological characteristics and produce force in a Ca^{2+}-dependent manner, but have specific force and rate of force development similar to neonatal myocardium, with passive stiffness similar to adult myocardium. Perhaps most significantly, this is the first report that NRC grafts can influence the calcium sensitivity of force development in uninjured myocardium far from the infarct region (Figure 4). Since the remote non-infarcted myocardium is orders of magnitude larger than the grafts, enhanced Ca^{2+} sensitivity in this region may be a major contributor to the improvement in global heart function.

Ca^{2+} Activated Force

Because contractile assessments were made on demembranated tissue (lacking the sarcolemma and sarcoplasmic reticulum), the increased Ca^{2+} sensitivity of remote myocardium from grafted hearts was independent of changes in intracellular Ca^{2+} transients. Additionally, we found that grafts induced no differences in myofilament protein isoforms in remote non-infarcted myocardium. Instead, enhanced Ca^{2+} sensitivity of remote myocardium from grafted hearts correlated with post-translational modification of myofilament proteins. Overall phosphorylation of myofilaments proteins was decreased in all infarcted groups, but we found that phosphorylation of TnT, Tm and MLC-2 was lower in myocardium from grafted hearts (remote and graft), as compared to non-treated infarcted hearts (Figure 5E). This reduced phosphorylation pattern is a likely candidate to at least partially account for the improvements in Ca^{2+} responsiveness, as it is known that phosphorylation of TnI, TnT, MLC or MyBP-C can affect the Ca^{2+} sensitivity of force in cardiac muscle (reviewed in [31]). Lower phosphorylation could result from reduced kinase activity and/or increased phosphatase activity. It is interesting to note that the three myofibrillar proteins TnT, Tm, and MLC with observed altered phosphorylation levels in myocardium from grafted hearts are targets for PKC. This is especially important in light of studies that have shown increased PKC activity to be associated with heart failure [32-34]. Alternatively, increased phosphatase activity could result in the reduced protein phosphorylation (as compared to sham), since all infarcted groups showed reduced overall protein phosphorylation, with cell-treated groups exhibiting even greater reductions. As such, it may be that the functional changes arise from the overall extent of dephosphorylation rather than the specific proteins. Overall, decreased phosphorylation of these three myofilament proteins seems a possible explanation, at least in part, for increased Ca^{2+} sensitivity observed in grafts and in remote myocardium from grafted infarcted hearts. Several studies have reported a decrease in F_{max} of skinned cardiomyocytes following an infarct [35-37], while others have shown no change [38, 39], or a slight increase [40, 41], similar to our results. Similarly, reports of changes in Ca^{2+} sensitivity of force are variable, with some reporting increases [35, 37], decreases [36, 39], or no change [40]. Between these studies there is no clear correlative pattern of phosphorylation changes with mechanical properties following infarction. Characterization of kinase and phosphatase levels to determine the signaling pathways for the observed altered phosphorylation levels certainly merits further study, as the differences in phosphorylation patterns are likely differentially affected by the type and severity of heart failure, as well as the type of treatment. It is also possible that Ca^{2+} sensitivity is being affected by other post-translational modifications not measured in this study. These may include protein acetylation, which has also been associated with increased Ca^{2+} sensitivity [42], and myofilament associated histone proteins [43], as well as others. It seems likely that identification of responsible signaling pathways could lead to new therapeutic targets. For example, it might be possible to develop treatments that similarly enhance Ca^{2+}

sensitivity of surviving myocardium without the need for cell transplantation. Analysis of these pathways may be helpful in elucidating signals resulting in, or halting, progression to heart failure.

Passive Mechanical Properties

The two dominant contributors to passive tension in cardiac muscle are titin and collagen, with titin dominating at sarcomere lengths ~1.85 to 2.15 μm and collagen dominating above ~2.2 μm [44]. Initial sarcomere length in our myocardial preparations was set at ~2.2 μm (see online Methods) prior to the stretching protocol. Thus, our stress-strain studies primarily assessed the contributions of the collagen network. A major finding was that cardiomyocyte grafts had passive stiffness properties similar to adult myocardium, while scar tissue was an order of magnitude stiffer. Qualitatively similar improvements in local infarct compliance have been reported following transplantation of human mesenchymal stem cells into rat infarcts [45]. The high degree of compliance in the graft region was surprising, given that graft samples contained only 30% less collagen than did scar tissue. Qualitative differences in collagen architecture may contribute to these differences. Whittaker *et al.* [46] showed that collagen fibers surrounding cardiomyocyte grafts form a disorganized woven network, whereas those in scar tissue form highly organized linear cables. A woven network can stretch due to deformation without stretching individual fibers, whereas tension on aligned cables places the load directly on the fibers themselves. Alternatively, there may be lower collagen cross-linking in the grafts, making them more compliant. It is interesting that grafts showed greater elastic recoil after stretch than either normal myocardium or scar (Figure 6D). This might contribute to ejection after diastolic stretch, or to diastolic recoil if the region exhibited systolic dyskenesis.

Physiological Implications of Enhanced Ca^{2+} Sensitivity

The physiological consequences of increased Ca^{2+} sensitivity in the remote myocardium will clearly depend on what happens to Ca^{2+} cycling in this region. It is important to highlight that the heart works at $[Ca^{2+}]$ levels around pCa_{50}, thus the increased Ca^{2+} sensitivity observed in remote myocardium from grafted hearts could have profound physiological implications. If Ca^{2+} transients in remote myocardium from grafted hearts are unchanged compared to non-treated infarcted hearts, we would predict greater systolic force generation. This would contribute to the enhanced global cardiac performance seen after NRC transplantation. Additionally, enhanced Ca^{2+} sensitivity of remote myocardium from grafted infarcted hearts would allow for comparatively greater force generation with smaller Ca^{2+} transients, thereby increasing ventricular efficiency. On the other hand, increased Ca^{2+} sensitivity may be a double edged sword that could impair relaxation. This impairment may in turn be ameliorated by the improvement in compliance in the graft area. The question also remains as to whether a chronic increase in Ca^{2+} sensitivity would eventually affect Ca^{2+} transients or lead to alterations in Ca^{2+} dependent signaling, such as through calcineurin, calcium/calmodulin dependent kinase, or PKC.

Potential Mechanisms

A key question is how do cardiomyocyte grafts in the infarct influence myofilament phosphorylation patterns in the non-infarcted region? We propose that the grafts initially exert a beneficial effect on the local infarct environment, which then reduces global mechanical and/or neurohumoral stress, leading to downstream alterations in myofilament kinase or phosphatase activity. Possible mechanisms through which local benefits could occur include direct graft systolic force generation, mechanical buttressing through wall thickening [47] and paracrine effects that promote vascularization and survival of cells in the border zone [6]. The isolation of NRC grafts by infarct fibrosis and the relative distant location from the remote myocardium suggest paracrine effects are unlikely to be solely responsible for the improved

cardiac function observed in cell-transplanted animals. Wall *et al.*[47] used a finite element model of an anterioapical infarcted LV to examine the short-term effect of injecting material into the LV wall. From their simulations, these investigators concluded that addition of non-contractile material to a damaged LV wall had important effects on cardiac mechanics. It is possible that cardiomyocyte transplantation indirectly increases the Ca^{2+} sensitivity of remote myocardium by altering the geometry and load of the heart, which could attenuate the remodeling process and perhaps induce myofilament protein isoform switches (not seen in this study) or changes in protein phosphorylation levels. The fact that several studies have shown enhanced function of injured hearts following transplantion of non-myogenic cell types (such as fibroblast, smooth muscle cells and mesenchymal stem cells)[48-50] clearly suggest that non-contractile effects may play a significant role in cell-based repair.

Summary

A number of groups have shown that transplantation of many cell types, including fetal and neonatal cardiomyocytes, improves function of the infarcted heart ([4,51] and reviewed in [2,3,7]). In agreement with those studies, here we found systolic fractional shortening was significantly increased in cell-treated infarcted hearts as compared to non-treated infarcted hearts (Figure 1). In most studies, however, cardiomyocyte grafts have been small, averaging <10% of the infarct region [11]. When one then considers that grafts can generate only ~10% of the maximal force of normal myocardium (Figure 4), this suggests that grafts should only contribute ~1% of the active force as compared to tissue lost to infarction. This alone is not sufficient to explain increased global contractile function. Our results with NRC grafts are the first to implicate their capacity to contribute both directly to systolic function in the infarct region and indirectly by influencing the contractile properties of remote myocardium. Because the remote myocardium typically accounts for >70% of the infarcted left ventricular mass, contractile changes in this region can readily translate to changes in global heart function.

Supplementary Material

Refer to Web version on PubMed Central for supplementary material.

Acknowledgments

The authors would like to thank Drs. Lil Pabon and Michael Laflamme for helpful scientific discussion and Dr. Elina Minami for training in animal surgery and echocardiography. We are indebted to Veronica Muskheli for her technical support in histology and TEM. We would like to thank Charles Luo for technical assistance in protein profile determination, Mark Schrader for technical assistance with force measurements, and Kellii Schrub and Sarah Dupras for assistance in animal surgery.

Sources of funding: This study was supported by National Institutes of Health Grants R21HL64387 (to M.R. and C.E.M), R01HL61683 (to M.R.), R01HL61553, P01HL03174, R01HL084642 (to CEM); and by American Heart Association grants AHA0510107Z (to A.M.G) and AHA0140040N (to M.R.)

References

1. Reffelmann T, Kloner RA. Cellular cardiomyoplasty--cardiomyocytes, skeletal myoblasts, or stem cells for regenerating myocardium and treatment of heart failure. Cardiovasc Res 2003 May 1;58(2): 358–68. [PubMed: 12757870]
2. Murry CE, Field LJ, Menasche P. Cell-based cardiac repair: reflections at the 10-year point. Circulation 2005 Nov 15;112(20):3174–83. [PubMed: 16286608]
3. Laflamme MA, Murry CE. Regenerating the heart. Nat Biotechnol 2005 Jul;23(7):845–56. [PubMed: 16003373]
4. Li RK, Jia ZQ, Weisel RD, Mickle DA, Zhang J, Mohabeer MK, et al. Cardiomyocyte transplantation improves heart function. Ann Thorac Surg 1996 Sep;62(3):654–60. [PubMed: 8783989]discussion 60-1

5. Sakai T, Li RK, Weisel RD, Mickle DA, Jia ZQ, Tomita S, et al. Fetal cell transplantation: a comparison of three cell types. J Thorac Cardiovasc Surg 1999 Oct;118(4):715–24. [PubMed: 10504639]
6. Muller-Ehmsen J, Peterson KL, Kedes L, Whittaker P, Dow JS, Long TI, et al. Rebuilding a damaged heart: long-term survival of transplanted neonatal rat cardiomyocytes after myocardial infarction and effect on cardiac function. Circulation 2002;105:1720–6. [PubMed: 11940553]
7. Laflamme MA, Zbinden S, Epstein SE, MC E. Cell-based therapy for myocardial ischemia and infarction: pathophysiological mechanisms. Annu Rev Pathol Mech Dis 2007;2:307–39.
8. Reinecke H, Murry CE. Cell grafting for cardiac repair. Methods in Molecular Biology 2003;219:97–112. [PubMed: 12597001]
9. Ismail JA, Poppa V, Kemper LE, Scatena M, Giachelli CM, Coffin JD, et al. Immunohistologic labeling of murine endothelium. Cardiovasc Pathol 2003 Mar-Apr;12(2):82–90. [PubMed: 12684163]
10. Etzion S, Battler A, Barbash IM, Cagnano E, Zarin P, Granot Y, et al. Influence of embryonic cardiomyocyte transplantation on the progression of heart failure in a rat model of extensive myocardial infarction. J Mol Cell Cardiol 2001 Jul;33(7):1321–30. [PubMed: 11437538]
11. Laflamme MA, Chen KY, Naumova AV, Muskheli V, Fugate JA, Dupras SK, et al. Cardiomyocytes derived from human embryonic stem cells in pro-survival factors enhance function of infarcted rat hearts. Nat Biotechnol 2007 Sep;25(9):1015–24. [PubMed: 17721512]
12. Chase PB, Kushmerick MJ. Effects of pH on contraction of rabbit fast and slow skeletal muscle fibers. Biophys J 1988 Jun;53(6):935–46. [PubMed: 2969265]
13. Regnier M, Rivera AJ, Wang CK, Bates MA, Chase PB, Gordon AM. Thin filament near-neighbour regulatory unit interactions affect rabbit skeletal muscle steady-state force-Ca(2+) relations. J Physiol 2002 Apr 15;540(Pt 2):485–97. [PubMed: 11956338]
14. Messer AE, Jacques AM, Marston SB. Troponin phosphorylation and regulatory function in human heart muscle: dephosphorylation of Ser23/24 on troponin I could account for the contractile defect in end-stage heart failure. J Mol Cell Cardiol 2007 Jan;42(1):247–59. [PubMed: 17081561]
15. Muller-Ehmsen J, Whittaker P, Kloner RA, Dow JS, Sakoda T, Long TI, et al. Survival and development of neonatal rat cardiomyocytes transplanted into adult myocardium. J Mol Cell Cardiol 2002 Feb;34(2):107–16. [PubMed: 11851351]
16. Scorsin M, Hagege AA, Marotte F, Mirochnik N, Copin H, Barnoux M, et al. Does transplantation of cardiomyocytes improve function of infarcted myocardium. Circulation 1997 Nov 4;96(9 Suppl):II-188–93.
17. Huwer H, Winning J, Vollmar B, Welter C, Lohbach C, Menger MD, et al. Long-term cell survival and hemodynamic improvements after neonatal cardiomyocyte and satellite cell transplantation into healed myocardial cryoinfarcted lesions in rats. Cell Transplant 2003;12(7):757–67. [PubMed: 14653622]
18. Prakash YS, Cody MJ, Housmans PR, Hannon JD, Sieck GC. Comparison of cross-bridge cycling kinetics in neonatal vs. adult rat ventricular muscle. J Muscle Res Cell Motil 1999 Oct;20(7):717–23. [PubMed: 10672520]
19. Reiser PJ, Westfall MV, Schiaffino S, Solaro RJ. Tension production and thin-filament protein isoforms in developing rat myocardium. Am J Physiol 1994 Oct;267(4 Pt 2):H1589–96. [PubMed: 7943406]
20. Korte FS, Herron TJ, Rovetto MJ, McDonald KS. Power output is linearly related to MyHC content in rat skinned myocytes and isolated working hearts. Am J Physiol Heart Circ Physiol 2005 August 1;289(2):H801–12. [PubMed: 15792987]
21. Fitzsimons DP, Patel JR, Moss RL. Role of myosin heavy chain composition in kinetics of force development and relaxation in rat myocardium. J Physiol Lond 1998;513:171–83. [PubMed: 9782168]
22. Cappelli V, Bottinelli R, Poggesi C, Moggio R, Reggiani C. Shortening velocity and myosin and myofibrillar ATPase activity related to myosin isoenzyme composition during postnatal development in rat myocardium. Circ Res 1989 Aug;65(2):446–57. [PubMed: 2526695]
23. Schillinger W, Kogler H. Altered phosphorylation and Ca2+-sensitivity of myofilaments in human heart failure. Cardiovasc Res 2003 Jan;57(1):5–7. [PubMed: 12504808]

24. van der Velden J, Papp Z, Zaremba R, Boontje NM, de Jong JW, Owen VJ, et al. Increased Ca2+-sensitivity of the contractile apparatus in end-stage human heart failure results from altered phosphorylation of contractile proteins. Cardiovasc Res 2003 Jan;57(1):37–47. [PubMed: 12504812]
25. Bilchick KC, Duncan JG, Ravi R, Takimoto E, Champion HC, Gao WD, et al. Heart failure-associated alterations in troponin I phosphorylation impair ventricular relaxation-afterload and force-frequency responses and systolic function. Am J Physiol Heart Circ Physiol 2007 Jan;292(1):H318–25. [PubMed: 16936010]
26. Noland TA Jr, Kuo JF. Phosphorylation of cardiac myosin light chain 2 by protein kinase C and myosin light chain kinase increases Ca(2+)-stimulated actomyosin MgATPase activity. Biochem Biophys Res Commun 1993 May 28;193(1):254–60. [PubMed: 8503915]
27. Lahmers S, Wu Y, Call DR, Labeit S, Granzier H. Developmental control of titin isoform expression and passive stiffness in fetal and neonatal myocardium. Circ Res 2004 Mar 5;94(4):505–13. [PubMed: 14707027]
28. Whittaker P. Collagen organization in wound healing after myocardial injury. Basic Res Cardiol 1998;93:23–5. [PubMed: 9879440]
29. Sicard RE, Werner JC. Dexamethasone-induced histopathology of neonatal rat myocardium. In Vivo 1994 May-Jun;8(3):353–8. [PubMed: 7803717]
30. Cleutjens JP, Creemers EE. Integration of concepts: Cardiac extracellular matrix remodeling after myocardial infarction. J Card Fail 2002 Dec;8(6 Suppl):S344–8. [PubMed: 12555143]
31. Page, E.; Fozzard, HA.; Solaro, RJ. Handbook of Physiology, Section 2: The Cardiovascular System, Vol I: The Heart. Vol. 1st. An American Physiological Society Book; 2001.
32. Wang J, Liu X, Sentex E, Takeda N, Dhalla NS. Increased expression of protein kinase C isoforms in heart failure due to myocardial infarction. Am J Physiol Heart Circ Physiol 2003 Jun;284 (6):H2277–87. [PubMed: 12742831]
33. Bowling N, Walsh RA, Song G, Estridge T, Sandusky GE, Fouts RL, et al. Increased protein kinase C activity and expression of Ca2+-sensitive isoforms in the failing human heart. Circulation 1999 Jan 26;99(3):384–91. [PubMed: 9918525]
34. Murphy S, Frishman WH. Protein kinase C in cardiac disease and as a potential therapeutic target. Cardiology in review 2005 Jan-Feb;13(1):3–12. [PubMed: 15596021]
35. Van der Velden J, Merkus D, Klarenbeek BR, James AT, Boontje NM, Dekkers DHW, et al. Alterations in myofilament function contribute to left ventricular dysfunction in pigs early after myocardial infarction. Circ Res 2004;95:e85–e95. [PubMed: 15528471]
36. Belin RJ, Sumandea MP, Kobayashi T, Walker LA, Rundell VL, Urboniene D, et al. Left ventricular myofilament dysfunction in rat experimental hypertrophy and congestive heart failure. Am J Physiol Heart Circ Physiol 2006;291(5):H2344–53. [PubMed: 16815982]
37. de Waard MC, van der Velden J, Bito V, Ozdemir S, Biesmans L, Boontje NM, et al. Early exercise training normalized myofilament function and attenuates left ventricular pump dysfunction in mice with a large myocardial infarction. Circ Res 2007;100(7):1079–88. [PubMed: 17347478]
38. Mou YA, Reboul C, Andre L, Lacampagne A, Cazorla O. Late exercise training improves non-uniformity of transmural myocardial function in rats with ischaemic heart failure. Cardiovascular Research 2009;81(3):555–64. [PubMed: 18703535]
39. Li P, Hofmann PA, Li B, Malhotra A, Cheng W, Sonnenblick EH, et al. Myocardial infarction alters myofilament calcium sensitivity and mechanical behavior of myocytes. American Journal of Physiology 1997;272(1):H360–H70. [PubMed: 9038957]
40. Wagner KD, Theres H, Born A, Strube S, Wunderlich N, Pfitzer G, et al. Contractile function of papillary muscle from rats with different infarct size after beta-adrenergic blockade and ACE-inhibition. J Mol Cell Cardiol 1997 Nov;29(11):2941–51. [PubMed: 9405169]
41. Geenen DL, White TP, Lampman RM. Papillary mechanics and cardiac morphology of infarcted rat hearts after training. J Appl Physiol 1987;63(1):92–6. [PubMed: 3624152]
42. Gupta MP, Samant SA, Smith SH, Shroff SG. HDAC4 and PCAF bind to cardiac sarcomeres and play a role in regulating myofilament contractile activity. J Biol Chem 2008;283(15):10135–46. [PubMed: 18250163]
43. Martin AF, Ball K, Gao LZ, Kumar P, Solaro RJ. Identification and functional significance of troponin I isoforms in neonatal rat heart myofibrils. Circ Res 1991 Nov;69(5):1244–52. [PubMed: 1934354]

44. Granzier HL, Irving TC. Passive tension in cardiac muscle: Contribution of collagen, titin, microtubules, and intermediate filaments. Biophys J 1995;68:1027–44. [PubMed: 7756523]
45. Berry MF, Engler AJ, Woo YJ, Pirolli TJ, Bish LT, Jayasankar V, et al. Mesenchymal stem cell injection after myocardial infarction improves myocardial compliance. American Journal of Physiology 2006;290:H2196–H203. [PubMed: 16473959]
46. Whittaker P, Muller-Ehmsen J, Dow JS, Kedes LH, Kloner RA. Development of abnormal tissue architecture in transplanted neonatal rat myocytes. Ann Thorac Surg 2003 May;75(5):1450–6. [PubMed: 12735561]
47. Wall ST, Walker JC, Healy KE, Ratcliffe MB, Guccione JM. Theoretical impact of the injection of material into the myocardium: a finite element model simulation. Circulation 2006 Dec 12;114(24): 2627–35. [PubMed: 17130342]
48. Hutcheson KA, Atkins BZ, Hueman MT, Hopkins MB, Glower DD, Taylor DA. Comparison of benefits on myocardial performance of cellular cardiomyoplasty with skeletal myoblasts and fibroblasts. Cell Transplant 2000 May-Jun;9(3):359–68. [PubMed: 10972335]
49. Fujii T, Yau TM, Weisel RD, Ohno N, Mickle DA, Shiono N, et al. Cell transplantation to prevent heart failure: a comparison of cell types. Ann Thorac Surg 2003 Dec;76(6):2062–70. [PubMed: 14667643]discussion 70
50. Berry MF, Engler AJ, Woo YJ, Pirolli TJ, Bish LT, Jayasankar V, et al. Mesenchymal stem cell injection after myocardial infarction improves myocardial compliance. Am J Physiol Heart Circ Physiol 2006 Jun;290(6):H2196–203. [PubMed: 16473959]
51. Sakai T, Li RK, Weisel RD, Mickle DA, Kim EJ, Tomita S, et al. Autologous heart cell transplantation improves cardiac function after myocardial injury. Ann Thorac Surg 1999 Dec;68(6):2074–80. [PubMed: 10616980]discussion 80-1

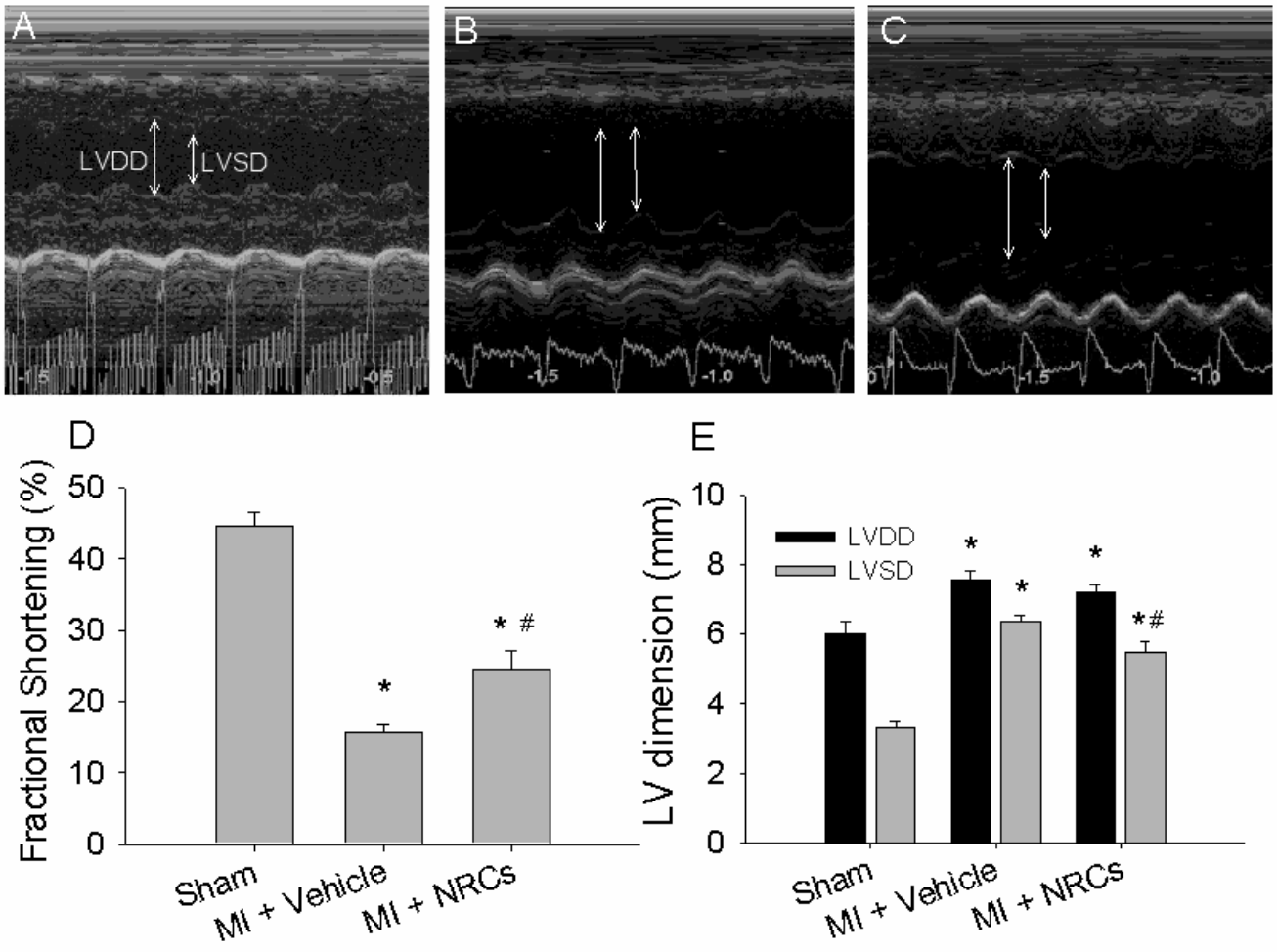

Figure 1. Assessment of myocardial function after cell transplantation by echocardiography

Representative left-ventricular M-mode images from control animals (**A**, sham, n = 6), and infarcted animals that received either vehicle (**B**, non-treated infarcted, n = 9) or cells (**C**, grafted, n =10). Arrows indicate chamber dimension at end-diastole (LVDD) and end-systole (LVSD). Fractional shortening (**D**) was greatly reduced with MI, but the functional decline was attenuated by cell transplantation. Both diastolic and systolic LV dimensions increased after MI (**E**). No difference was found in LV diastolic dimension (**E**, LVDD) between non-treated infarct or grafted hearts, but LV systolic dimension (**E**, LVSD) was reduced in grafted hearts. Values are means ± S.E.M.; * $p < 0.05$ versus sham; # $p < 0.05$ versus MI + vehicle.

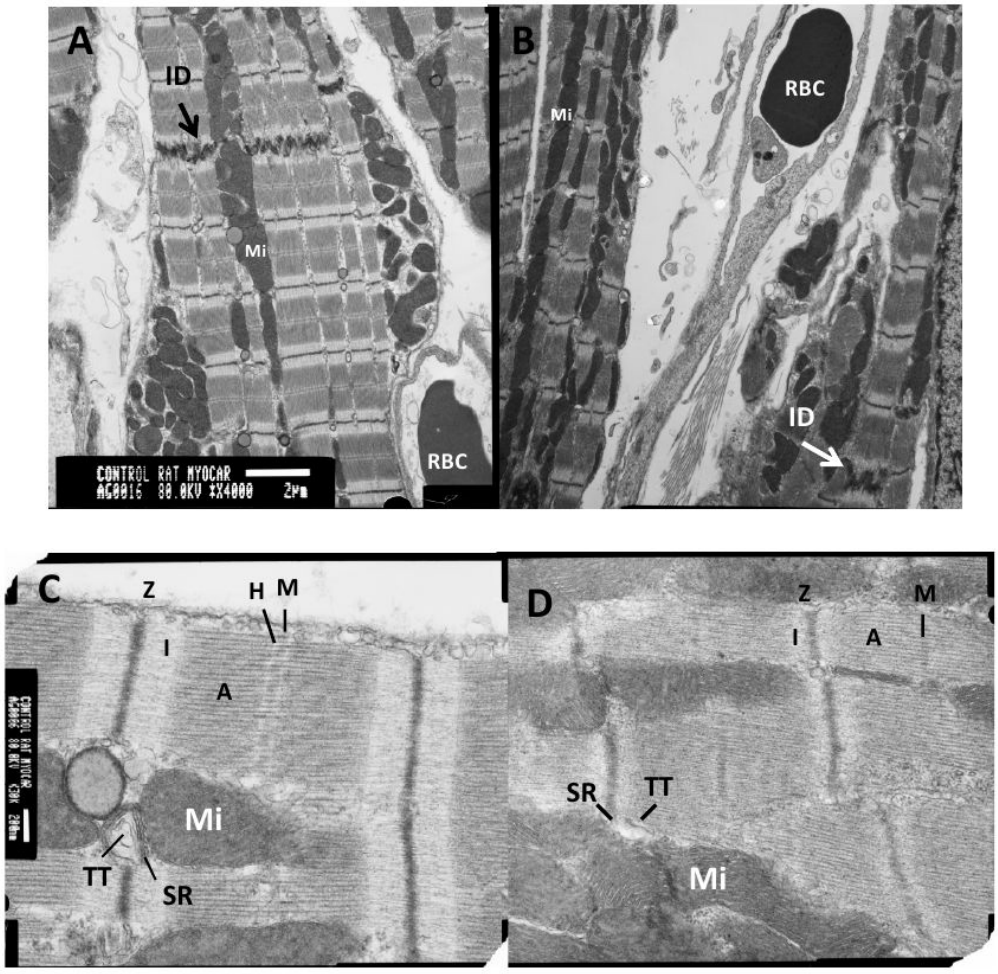

Figure 2. Transmission Electron Microscopy

Images of sham (**A, C**) and graft (**B, D**) myocardial tissue at equivalent magnification (scale bar in A = 2 μm; in B = 200 nm). Arrows in A and B indicate intercalated discs (ID). Images of tissue in C and D show M-lines (M), I bands (I), A bands (A), Z discs (Z), H zone (H), mitochondria (Mi), sarcoplasmic reticulum (SR), and T-tubules (TT). The graft cells show mature cardiac structure except for Z-disk misalignment.

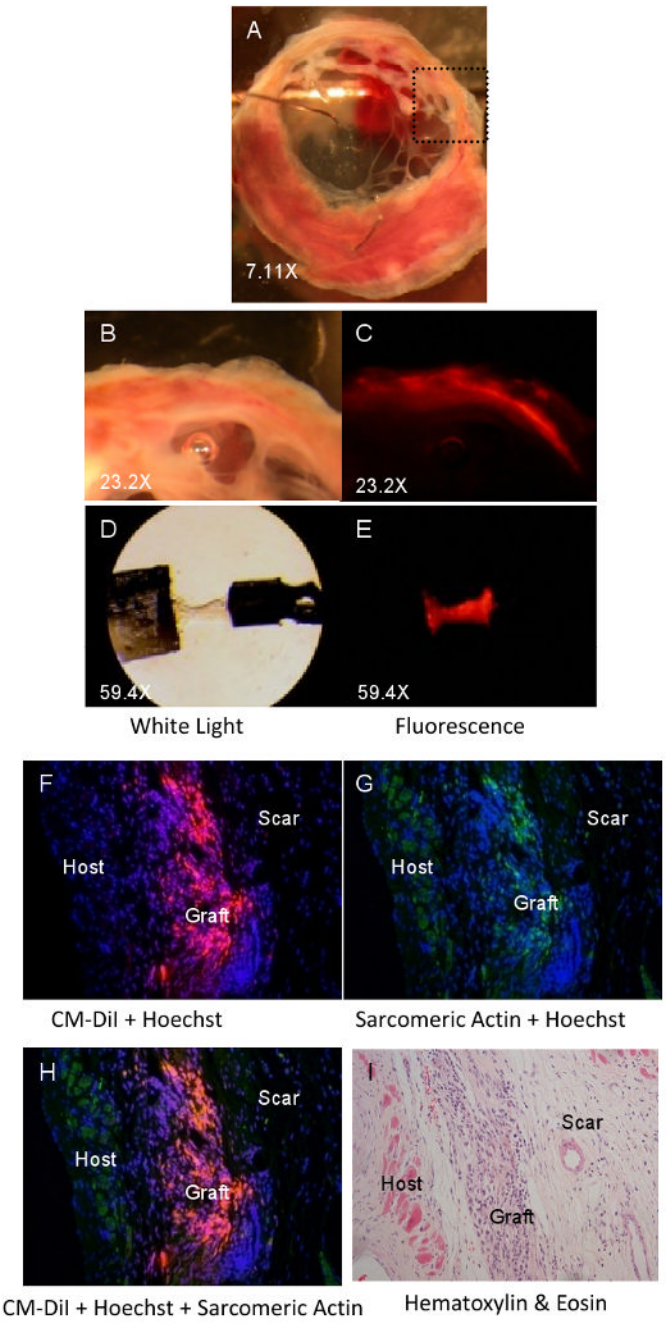

Figure 3. Tissue strip dissection and graft identification

(**A**) Example of myocardial slice containing grafted CM-DiI-labeled cells eight weeks after transplantation. Higher magnification of the boxed region of interest (in A) under white light (**B**) and fluorescent light (rhodamine filter) (**C**) shows CM-DiI positive tissue. **D**) Example of muscle strip dissected from an infarcted heart eight weeks after CM-DiI-labeled NRC transplantation (0.7 mm × 166 μm × 200 μm). CM-DiI-positive tissue can be observed in the tissue strip under fluorescent light (**E**). CM-DiI (red, **F**) identifies transplanted cardiomyocytes (sarcomeric actin, green, **G**) in infarcted hearts up to eight weeks after cell transplantation. **H**) Merge of F and G. Nuclei were counterstained with Hoechst 33342. **I**) H&E stain of consecutive slide shows morphology of transplanted cells. Magnification 20×.

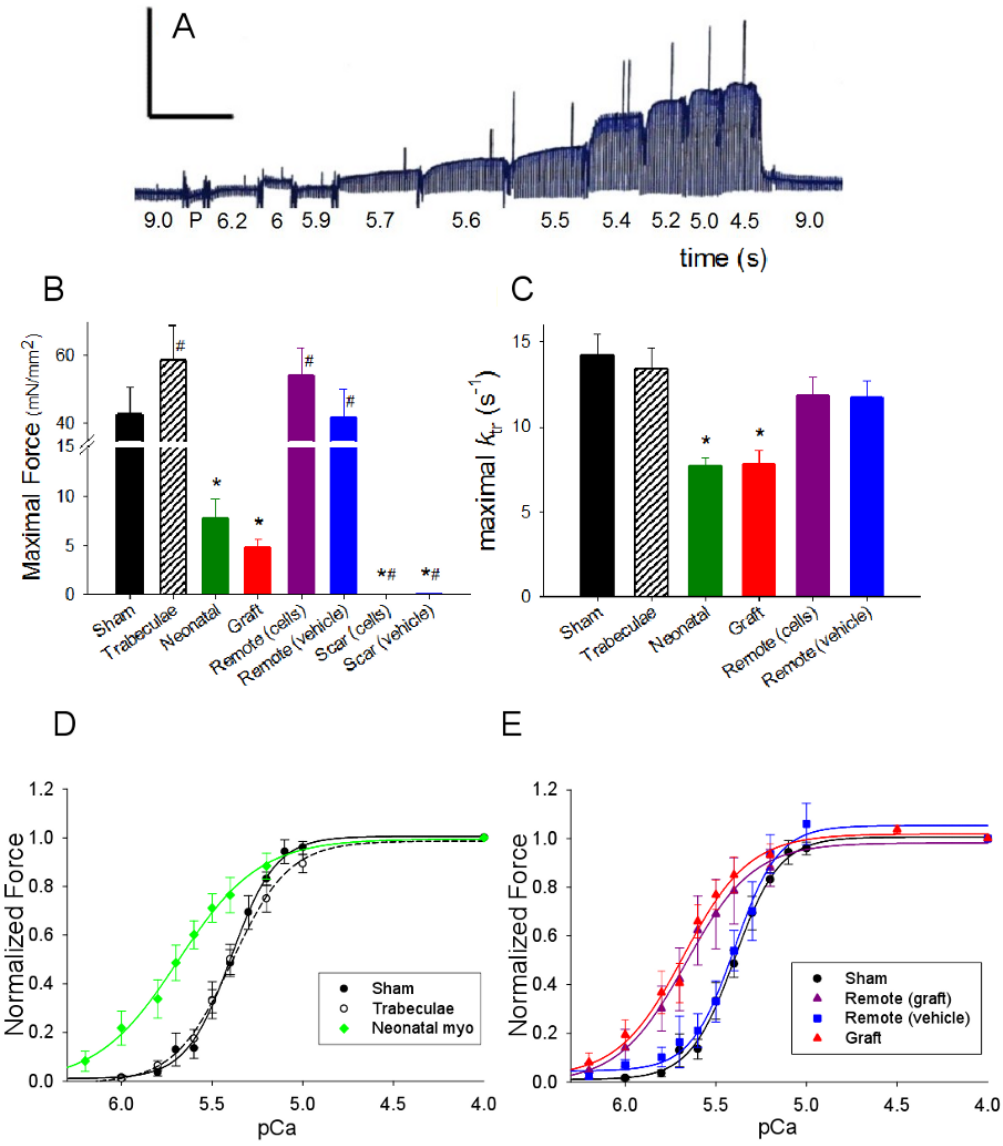

Figure 4. Ca^{2+} activated force

(**A**). Example record of force-pCa protocol. [Ca^{2+}] was varied as indicated and isometric force was measured at steady-st, ate. For this example sham strip Fmax = 48.4 mN/mm^2, pCa_{50} = 5.41 ± 0.01, n_H = 3.2 ± 0.1 and the muscle dimensions were 1.5 mm (length) and 256 μm (width/thickness). Scale bar: 48 mN/mm2 (y-axis) and 150 s (x-axis). Summary bar plots of Fmax (**B**) and ktr (**C**) for all groups. Summary force-pCa data of controls (**D**) and grafted and non-treated infarcted (**E**) groups. Sham data are shown in D and E for comparison with experimental strips. Values are means ± S.E.M. (see Table 1 for all values)

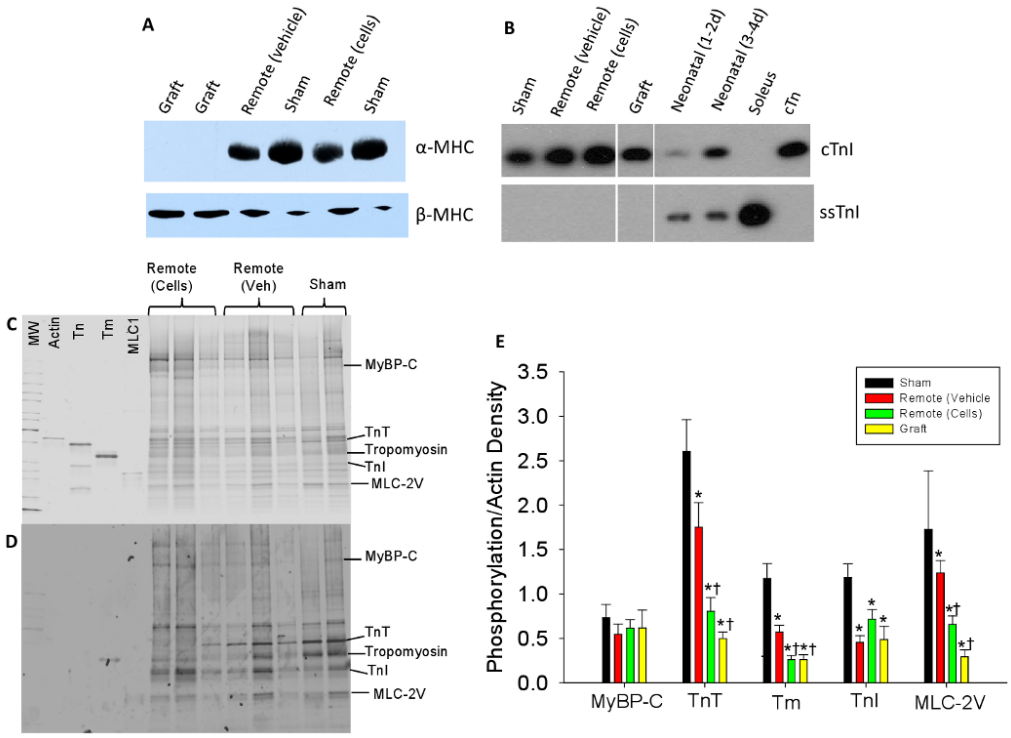

Figure 5. Protein Profiling

Representative western blot for α-MHC and β-MHC (**A**) and cTnI and ssTnI (**B**). **C**) Gray-scaled coomassie blue total protein stain and **D**). Pro-Q-diamond stain against phosphoproteins from sham hearts, remote tissue from grafted hearts (+) and remote tissue from non-treated infarcted hearts (-). Gel contains molecular weight markers (MW), and purified proteins actin, troponin complex (Tn), tropomyosin (Tm), and MLC1 for orientation. **D**) Quantification of phosphoprotein staining for all groups normalized for protein load (actin density) and to sham-operated myocardium. * $p < 0.05$ versus sham and † $p < 0.05$ versus remote (vehicle).

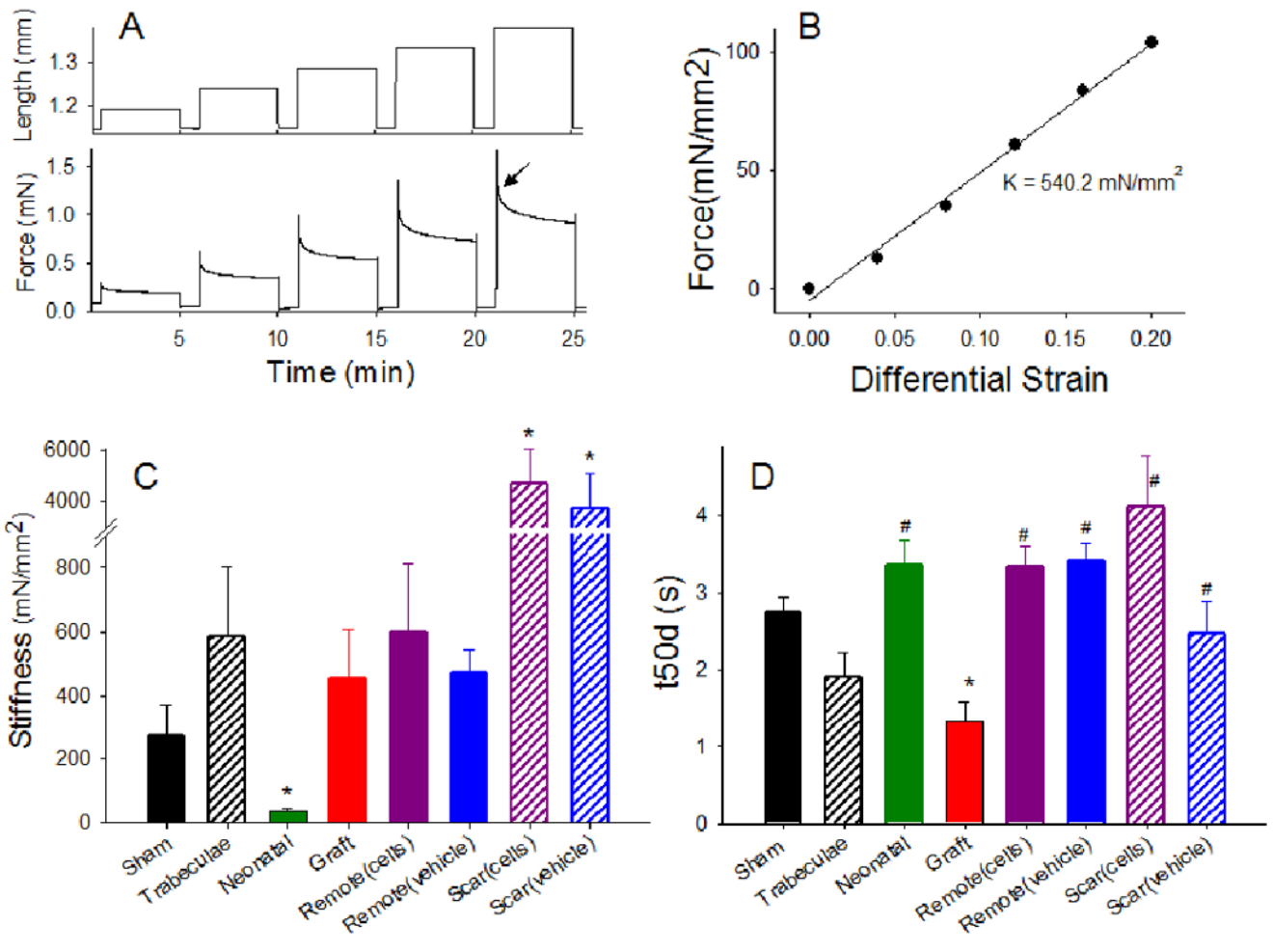

Figure 6. Passive mechanics

A) Example length and passive force trace of a strip to determine the stress-strain relation. Arrow indicates force after 50% decay. The strip is stretched from L_0 in 4% increments up to 1.20 L_0. Each length is held for 4 min, followed by 1 min rest. The stiffness constant is then calculated as the slope of the maximal passive force vs. differential strain (DS) relation (**B**). Stiffness constant (**C**) and time after 50% force decay (t50d) (**D**) of strips from all study groups (see Table 1 for values). Values are means ± S.E.M. In C,* $p < 0.05$ versus sham or graft. In D, * $p < 0.05$ versus sham and # $p < 0.05$ versus graft.

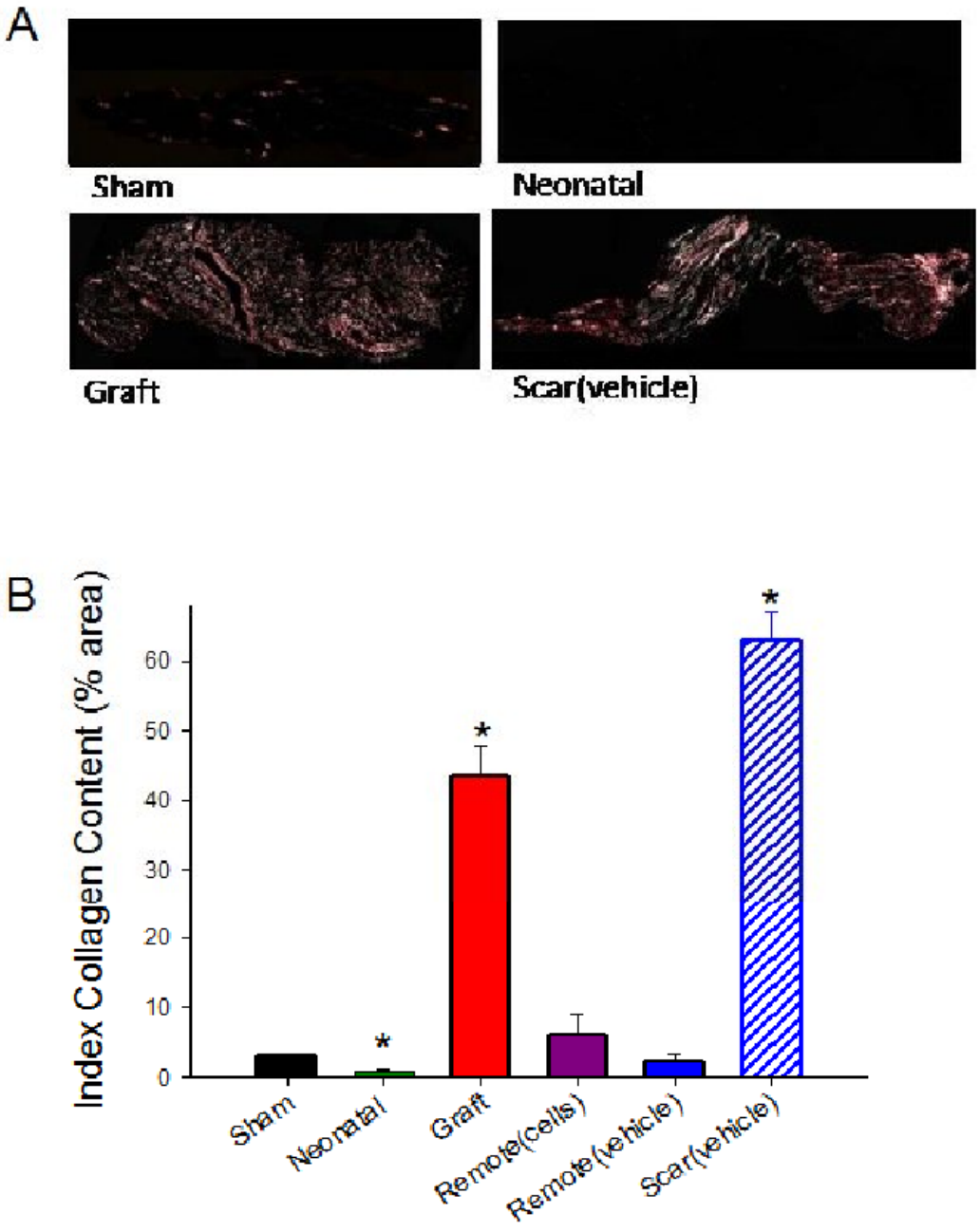

Figure 7. Quantification of collagen content

A) Example images of sham, neonatal, scar, and graft strips stained with picrosirius red/fast green and viewed under linear polarized light. Note the clear differences in the percent area positive for collagen (pink) are observed. Magnification 10×. **B**) Quantification of the % area in the strips positive for collagen (see Table 1 for values). Values are means ± S.E.M; * $p < 0.05$ versus sham.

Table 1

Summary of dimensions, biochemical and histological parameters of muscle strips in different study groups

(# preps)	Sham	Trabeculae	Neonatal	Graft	Remote (grafted)	Remote (non-treated)	Scar (near graft)	Scar (vehicle)
Length (mm)	1.1 ± 0.1 (14)	1.0 ± 0.1 (16)	1.4 ± 0.1 (23)	0.9 ± 0.1 (10)	1.1 ± 0.04 (17)	1.0 ± 0.1 (13)	0.9 ± 0.1 (6)	1.1 ± 0.1 (10)
Width (μm)	197.8 ± 10.6 (14)	172.2 ± 20.8 (16)	235.2 ± 12.9 (23)	183.5 ± 6.9 (10)	216.4 ± 8.5 (17)	189.1 ± 10.6 (13)	196.2 ± 13.9 (6)	171.6 ± 15.1 (10)
Thickness (μm)	199.3 ± 18.4 (13)	n.a.	148.3 ± 4.1 (20)	197.2 ± 10.1 (10)	219.7 ± 6.2 (17)	193.8 ± 10.8 (12)	171.3 ± 22.0 (6)	209.7 ± 10.9 (9)
F_{max} (mN/mm^2)	42.8 ± 8.0 (14)	58.6 ± 10.2 (12)	7.8 ± 1.9 (21)	4.7 ± 0.9 (8)	54.1 ± 8.2 (7)	41.8 ± 8.4 (13)	0.0 ± 0.0 (5)	0.1 ± 0.1 (10)
Maximal k_{tr} (s^{-1})	14.2 ± 1.3 (14)	13.4 ± 1.2 (12)	7.7 ± 0.5 (19)	7.8 ± 0.8 (8)	11.8 ± 1.1 (7)	11.7 ± 1.0 (13)	n.a.	n.a.
pCa_{50}	5.41 ± 0.03 (14)	5.39 ± 0.04 (7)	5.70 ± 0.06 (7)	5.69 ± 0.07 (6)	5.64 ± 0.10 (7)	5.45 ± 0.04 (12)	n.a.	n.a.
n_H	5.0 ± 0.6 (14)	3.0 ± 0.2 (7)	2.1 ± 0.2 (7)	3.5 ± 0.8 (6)	2.5 ± 0.2 (7)	5.8 ± 0.9 (12)	n.a.	n.a.
Stiffness (mN/mm^2)	273.3 ± 100.1 (4)	585.6 ± 216.7 (7)	38.5 ± 9.1 (17)	452.8 ± 155.5 (8)	596.1 ± 213.0 (12)	469.5 ± 75.9 (11)	4676.2 ± 1380.3 (5)	3730.4 ± 1339.8 (9)
Passive F_{max} (mN/mm^2)	54.7 ± 20.1 (4)	119.8 ± 43.3 (7)	7.6 ± 1.8 (17)	90.0 ± 32.1 (8)	119.8 ± 44.2 (12)	91.4 ± 14.6 (11)	920.9 ± 274.2 (5)	736.4 ± 259.6 (9)
Passive force at 4-min (mN/mm^2)	29.4 ± 11.3 (4)	59.5 ± 23.2 (7)	4.4 ± 1.2 (17)	33.8 ± 11.4 (8)	61.0 ± 20.1 (12)	51.4 ± 8.0 (11)	618.8 ± 220.9 (5)	409.7 ± 156.6 (9)
t50d (s)	2.7 ± 0.2 (4)	1.9 ± 0.3 (6)	3.4 ± 0.3 (13)	1.3 ± 0.3 (8)	3.3 ± 0.3 (12)	3.4 ± 0.2 (11)	4.1 ± 0.7 (5)	2.5 ± 0.4 (9)
% collagen area	3.1 ± 0.3 (4)	n.a.	0.8 ± 0.2 (5)	43.5 ± 4.4 (11)	6.0 ± 3.0 (4)	2.1 ± 1.2 (4)	n.a.	62.9 ± 4.1 (5)

J Mol Cell Cardiol. Author manuscript; available in PMC 2010 November 1.